Catalytic Strategy of *S*-Adenosyl-L-homocysteine Hydrolase: Transition-State Stabilization and the Avoidance of Abortive Reactions†

Xiaoda Yang,[‡,§] Yongbo Hu,[‡,||] Daniel H. Yin,[‡,⊥] Mary A. Turner,[▽] Mengmeng Wang,[○] Ronald T. Borchardt,[‡] P. Lynne Howell,[▽,#] Krzysztof Kuczera,[○] and Richard L. Schowen*[,‡,○]

Departments of Pharmaceutical Chemistry and Molecular Biosciences, The University of Kansas, Lawrence, Kansas 66047, Program in Structural Biology and Biochemistry, Research Institute, The Hospital for Sick Children, 555 University Avenue, Toronto, M5G 1X8 Ontario, Canada, and Department of Biochemistry, University of Toronto, Toronto, M5S 1A8 Ontario, Canada

Received June 4, 2002; Revised Manuscript Received December 15, 2002

ABSTRACT: *S*-Adenosylhomocysteine hydrolase (AdoHcy hydrolase) crystallizes from solutions containing the intermediate analogue neplanocin A with the analogue bound in its 3′-keto form at the active sites of all of its four subunits and the four tightly bound cofactors in their reduced (NADH) state. The enzyme is in the closed conformation, which corresponds to the structure in which the catalytic chemistry occurs. Examination of the structure in the light of available, very detailed kinetic studies [Porter, D. J., Boyd, F. L. (1991) *J. Biol. Chem. 266*, 21616−21625. Porter, D. J., Boyd, F. L. (1992) *J. Biol. Chem. 267*, 3205−3213. Porter, D. J. (1998) *J. Biol. Chem. 268*, 66−73] suggests elements of the catalytic strategy of AdoHcy hydrolase for acceleration of the reversible conversion of AdoHcy to adenosine (Ado) and homocysteine (Hcy). The enzyme, each subunit of which possesses a substrate-binding domain that in the absence of substrate is in rapid motion relative to the tetrameric core of the enzyme, first binds substrate and ceases motion. Probably concurrently with oxidation of the substrate to its 3′-keto form, the closed active site is "sealed off" from the environment, as indicated by a large (10^{8-9}-fold) reduction in the rate of departure of ligands, a feature that prevents exposure of the labile 3′-keto intermediates to the aqueous environment. Elimination of the 5′-substituent (Hcy in the hydrolytic direction, water in the synthetic direction) generates the central intermediate 4′,5′-didehydro-5′-deoxy-3′-ketoadenosine. Abortive 3′-reduction of the central intermediate is prevented by a temporary suspension of all or part of the redox catalytic power of the enzyme during the existence of the central intermediate. The abortive reduction is 10^4-fold slower than the productive reductions at the ends of the catalytic cycle and has a rate constant similar to those of nonenzymic intramolecular model reactions. The mechanism for suspending the redox catalytic power appears to be a conformationally induced increase in the distance across which hydride transfer must occur between cofactor and substrate, the responsible conformational change again being that which "seals" the active site. The crystal structure reveals a well-defined chain of three water molecules leading from the active site to the subunit surface, which may serve as a relay for proton exchange between solvent and active site in the closed form of the enzyme, permitting maintenance of active-site functional groups in catalytically suitable protonation states.

S-Adenosylhomocysteine hydrolase (*1*; AdoHcy hydrolase,[1] EC 3.3.1.1) converts *S*-adenosylhomocysteine (AdoHcy) to adenosine (Ado) and homocysteine (Hcy) when operating in the *hydrolytic* direction and catalyzes the reverse reaction when operating in the *synthetic* direction. The action of AdoHcy hydrolase assists in the regulation of a number of *S*-adenosylmethionine-dependent transmethylation reactions, of which AdoHcy is a powerful product inhibitor. AdoHcy hydrolase also controls blood levels of homocysteine, which

† This work was supported by a grant from the National Institutes of Health (GM-29332).

* To whom correspondence should be addressed at the Department of Pharmaceutical Chemistry. Phone: (785) 864-4080. Fax: (785) 864-5736. E-mail: rschowen@ku.edu.

‡ Department of Pharmaceutical Chemistry, The University of Kansas.

§ Current address: Department of Chemical Biology, School of Pharmaceutical Science, Peking University Health Science Center, Beijing, China 10008.

|| Current address: Department of Biological Chemistry, Wyeth Research, Pearl River, NY 10965.

⊥ Current address: Department of Vaccine Pharmaceutical Research, Merck Research Laboratories, West Point, PA 19486.

▽ The Hospital for Sick Children.

○ Department of Molecular Biosciences, The University of Kansas.

University of Toronto.

[1] Abbreviations: A, adenosine or its concentration in kinetic equations; Ado, adenosine; AdoHcy, *S*-adenosylhomocysteine; AdoHcy hydrolase, *S*-adenosylhomocysteine hydrolase; C, closed form of AdoHcy hydrolase; D, 4′,5′-didehydro-5′-deoxyadenosine or its concentration in kinetic equations; D-eritadenine, 2(*R*),3(*R*)-dihydroxy-4-(9-adenyl)butyric acid; DFHHA, 6′-deoxy-6′-fluoro-5′-hydroxyhomoadenosine; DHCeA, 2′,3′-dihydroxycyclopentenyladenine; DK, 4′,5′-didehydro-5′-deoxy-3′-ketoadenosine or its concentration in kinetic equations; EDDFHA, (*E*)-5′,6′-didehydro-6′-deoxy-6′-fluorohomoadenosine; H, homocysteine or its concentration in kinetic equations; Hcy, homocysteine; IPTG, isopropyl-*β*-D-thiogalactopyranoside; KA, 3′-ketoadenosine or its concentration in kinetic equations; 3′-ketoAdo, 3′-ketoadenosine; KS, 3′-keto-*S*-adenosylhomocysteine or its concentra-

10.1021/bi0262350 CCC: $25.00
Published on Web 01/28/2003

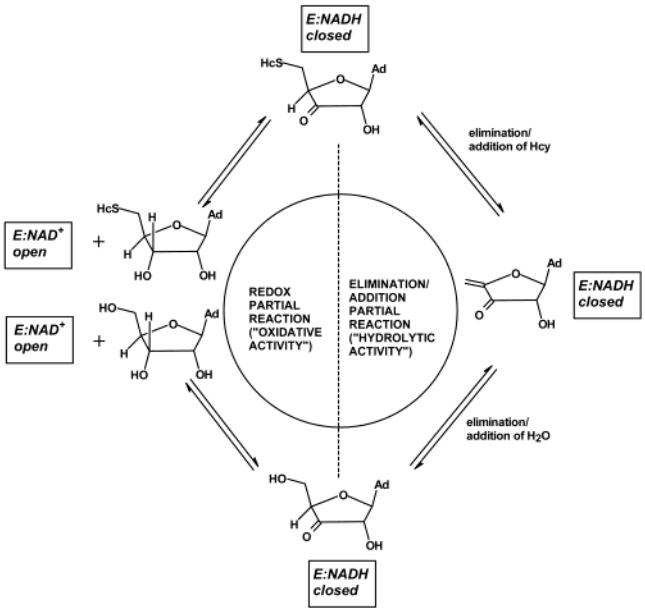

FIGURE 1: The catalytic cycle of AdoHcy hydrolase resolves into two partial reactions: a *redox partial reaction* occurring at the beginning and end of the cycle and thus spanning an *elimination/addition partial reaction*, which effects the fission/formation of the C-5′−S bond and the formation/fission of the C-5′−O bond. The free enzyme is in the NAD^+ form and possesses an *open structure* in which the substrate-binding and cofactor-binding domains are in relative motion. After binding of free substrate and oxidation, the enzyme is in the NADH form and possesses a *closed structure* in which the two domains are closed against each other to isolate the active site from the external environment.

appear to be risk factors for cardiovascular disease (*2*−*4*) and possibly amyloid diseases (*5*). The enzyme is a target for antiviral (*6*) and antiparasitic (*7*) drugs.

The mechanism of action of the enzyme (*1*) is shown in Figure 1. A redox partial reaction spans an elimination/addition partial reaction. The redox activity is dependent on an NAD^+ cofactor that in mammalian enzymes is bound with a near-nanomolar dissociation constant. The redox partial reaction comprises conversion of AdoHcy in the hydrolytic direction and Ado in the synthetic direction to the 3′-keto form at the beginning of the catalytic cycle and reduction of the 3′-keto form of the product to Ado in the hydrolytic direction and to AdoHcy in the synthetic direction at the end of the catalytic cycle. The intervening elimination/addition partial reaction is based on the lability of the 4′-CH bond in the 3′-keto form of the substrate. Removal of the 4′-hydrogen allows elimination of Hcy (hydrolytic direction), which is immediately released from the enzyme, or water (synthetic direction). Michael addition of the second substrate (water in the hydrolytic direction, Hcy in the synthetic direction) then completes the elimination/addition partial reaction.

Structurally, AdoHcy hydrolase is a homotetramer (*8*). The monomeric subunits resolve into three domains: a large N-terminal substrate-binding domain, a large cofactor-binding domain, and a smaller C-terminal "tail". The tail of subunit A protrudes into the adjacent subunit B and forms part of the cofactor-binding site in that subunit. There is a reciprocal penetration of the tail from subunit B into subunit A, forming part of the cofactor-binding site of subunit A. This linkage of subunits A and B is repeated in subunits C and D, but there is no similar linkage between the members of the AB pair and the members of the CD pair. The tetrameric AdoHcy hydrolase is therefore a "dimer of dimers". The four cofactor-binding domains together form a central core of the tetramer structure, with the substrate-binding domains exposed on the surface.

When the cofactor is in the oxidized (NAD^+) state and no substrate or substrate analogue is present, AdoHcy hydrolase crystallizes in the *open* conformation, in which an angle of 19° is formed by the inner surfaces of the two large domains (*9*). In this state, the substrate-binding domain oscillates with a frequency around 4×10^7 s^{-1} (*10*). Upon binding of a molecule of substrate or substrate analogue, the motion ceases (*10*), and in the case of 3′-oxidizable ligands, oxidation results with conversion of the ligand to the 3′-keto form and the cofactor to the NADH oxidation state. The enzyme is now in the *closed* state, in which the quaternary structure also differs from that in the open structure, the AB dimer having suffered a 14° rotation relative to the CD dimer (*1*).

In the present paper we address, with the aid of a new crystallographic structure, the questions of (a) how the enzyme achieves catalysis through stabilization of transition states while simultaneously avoiding the abortive reduction of the central dehydro keto intermediate and (b) how the abortive release or exposure to aqueous buffer of the hydrolytically labile keto intermediates is avoided.

MATERIALS AND METHODS

Crystallization of the Complex of AdoHcy Hydrolase with Neplanocin A and Crystallographic Data Collection and Processing. Recombinant human AdoHcy hydrolase purified from cell-free extracts of *E. coli* transformed with the plasmid pPROKcd20 (*11*) was used to prepare the pure apoprotein as described previously (*12*). This apoprotein was then incubated with NAD^+ to yield the pure NAD^+ form of the enzyme. The NAD^+ form of the enzyme was subsequently inactivated with neplanocin A (NepA), a type I mechanism-based inhibitor, forming the NepA-inactivated enzyme containing 1 equiv of NADH and 1 equiv of 3′ keto-NepA bound to each subunit of the protein.

Crystals of AdoHcy hydrolase complexed with 3′-keto-NepA (SAHH+NepA) were grown at room temperature by the hanging-drop vapor-diffusion method as previously described (*8*, *13*). Equal volumes (3 μL) of the protein (28 mg/mL) and of the precipitating solution (12% (w/v) PEG 4K, 20% (v/v) 2-propanol, 200 mM ammonium acetate, 100 mM citrate buffer, pH 5.6) were suspended over a 1.0 mL reservoir containing the same precipitating solution. The crystals grew as flat plates within a few days with average dimensions of $0.25 \times 0.15 \times 0.05$ mm. Prior to data collection, the SAHH+NepA crystals were soaked in cryoprotectant (21% (v/v) glycerol in precipitating solution) for 90 min, then transferred to a rayon CryoLoop (Hampton Research), and flash frozen in the cold stream. After initial characterization on our home source, the crystal was stored in liquid nitrogen for transportation. Data were subsequently

tion in kinetic equations; NepA, Neplanocin A; O, open form of AdoHcy hydrolase; S, *S*-adenosylhomocysteine or its concentration in kinetic equations; SAHH+NepA, *S*-adenosylhomocysteine hydrolase complexed with 3′-keto-NepA; W, water.

Table 1: Diffraction Collection and Refinement Statistics for the Crystallographic Structure

diffraction data		refinement statistics	
wavelength (Å)	0.97905	resolution (Å)	30 to 2.01
resolution (Å)	2.01	no. of reflns	34435
space group	*F*222	no. of protein atoms	3322
a (Å)	92.83	no. of solvent atoms	224
b (Å)	135.67	no. of NADH atoms	44
c (Å)	171.49	no. of inhibitor atoms	19
no. of measured reflns	201201	R_{cryst}/R_{free}[b]	19.7/23.6
no. of unique reflns	35337	rmsd[c] bond length (Å)	0.018
mean redundancy	5.7	rmsd bond angle (deg)	1.8
av $I/\sigma(I)$	18.5	dihedral angle (deg)	23.6
completeness[a] (%)	97.5 (91.4)	improper angle (deg)	1.23
$F^2 > 3\sigma(F^2)$[a] (%)	84.0 (56.0)	*B* factors (Å^2)	
R_{sym}[a]	0.051 (0.268)	protein	28.5
		solvent	31.3
		NADH	19.1
		inhibitor	19.2

[a] The values given in parentheses are the completeness and R_{sym} for the last resolution shell (2.08−2.01 Å). $R_{sym} = \sum\sum|I_i - \langle I\rangle|/\sum I_i$, where $\langle I\rangle$ is the average of equivalent reflections and the sum is extended over all measured observations for all unique reflections. [b] $R_{cryst} = \sum||F_o| - |F_c||/\sum|F_o|$, where F_o and F_c are the observed and calculated structure factors, respectively. For R_{free}, the sum is extended over a subset of reflections (10%) excluded from all stages of refinement. [c] rmsd = root-mean-square deviation.

collected at liquid nitrogen temperatures (100 K) at Station X8C, National Synchrotron Light Source, Brookhaven, Long Island. The crystal belonged to space group *F*222 and diffracted to ~2 Å resolution (Table 1). A total of 156 images with $\Delta\varphi = 1°$ were collected on a MAR Research (300 mm) image plate detector. All data were processed using DENZO/SCALEPACK (*14*). Final data reduction statistics are presented in Table 1.

Structure Determination and Refinement. The structure of the SAHH+NepA was solved by molecular replacement using the program CNS (*15*). A monomer of the AdoHcy hydrolase complexed with DHCeA (PDB accession code 1A7A) (*8*) was used as the search model for molecular replacement. Rotation functions were calculated in the resolution range of 15−4 Å. The final molecular replacement solution for the single monomer in the asymmetric unit had a correlation coefficient of 72.5% and a packing value of 50.86%. The structure was refined using the maximum likelihood target (*16*) implemented into CNS (*15*) with a flat bulk solvent correction and no σ cutoff applied to the data. Ten percent of the structure factors were randomly selected, excluded from the refinement, and used to compute R_{free} (*17*). Refinement of the model using the simulated annealing slow-cooling protocol (*18*, *19*) was alternated with manual inspection and rebuilding of the model using O (*20*). The final model for the monomer contains 430 amino acid residues, 1 NADH molecule, 1 inhibitor molecule, and 2 2-propanol molecules. A total of 216 water molecules obeying proper hydrogen bond geometry and with density greater than 3σ on σ_A-weighted $|F_o| - |F_c|$ maps were included in the model. The structure comprises amino acid residues 3−432. The quality of the electron density at the N-terminus prohibited the modeling of the first two residues. The final refinement statistics for the structure are presented in Table 1. Analysis of the structure by PROCHECK (*21*) showed that 90.1% of the non-glycine residues lie in the most favored regions of the Ramachandran plot and that no residues lie in the disallowed regions. The coordinates and structure factors have been deposited in the Protein Data Bank (PDB accession code 1LI4; RCS RCSB015962).

Kinetic and Equilibrium Constants of Porter and Boyd. To permit the construction of free-energy/reaction-progress diagrams, rate and equilibrium constants were taken from the thorough and exacting studies of Porter and Boyd (*22*−*24*). The values used and their corresponding free-energy changes are listed in Table 2.

Superposition of Open and Closed Structures of the Enzyme. The program QUANTA was used to superimpose each pair of structures. In each superposition, a sequence alignment was first performed on subunit A of the tetrameric enzyme. Next, residues of the NAD-binding domain (200−350 in the human enzyme) in one structure are overlaid on the corresponding residues in the other structure by minimizing the root-mean-square (RMS) deviation of backbone-atom positions through rigid-body rotation and translation. Finally, the distances between the selected atom pairs are measured in the overlaid structures using QUANTA.

There is currently available a single structure of AdoHcy hydrolase in the open conformation, a structure of the rat liver enzyme with each of the four cofactor-binding sites occupied by NAD^+ (*9*; 2.8 Å resolution; PDB code 1KY4). There are currently available four structures of AdoHcy hydrolase in the closed conformation, listed here by their PDB codes: 1A7A (*8*, 2.8 Å resolution), a complex of the human placental enzyme with each of the four cofactor-binding sites occupied by NADH and each of the four substrate-binding sites occupied by the 3′-keto form of the inhibitor DHCeA, thus a carbocyclic analogue of the intermediate 4′,5′-didehydro-5′-deoxy-3′-ketoadenosine;

1LI4 (this work; 2.0 Å resolution), a complex of the human placental enzyme with each of the four cofactor-binding sites occupied by NADH and each of the four substrate-binding sites occupied by the 3′-keto form of the inhibitor NepA, thus also a carbocyclic analogue of the intermediate 4′,5′-didehydro-5′-deoxy-3′-ketoadenosine;

1K0U (*25*; 3.0 Å resolution), a complex of the rat liver enzyme with each of the four cofactor-binding sites occupied by NAD^+ and each of the four substrate-binding sites occupied by the inhibitor D-eritadenine, an acyclic 4-adenyl-2,3-dihydroxybutanoic acid anion.

1KY5 (*26*, *33*; 2.8 Å resolution), a complex of the D244E mutant of the rat liver enzyme with weakly bound NADH and the 3′-keto form of the substrate adenosine in each of the four substrate-binding sites. In each case the occupancy of the NADH and 3′-ketoAdo moieties was refined to 50%. Superposed structures were constructed for the open form 1KY4 with each of the four closed-form structures.

Determination of Active-Site Cofactor Composition. AdoHcy hydrolase (42 μM, 2 mg/mL) was incubated with 100 μM DHCeA or NepA at room temperature overnight, leading to complete inactivation. The enzyme was denatured by addition of 2.5 volumes of ethanol, and the NAD/NADH composition was determined by the fluorescence method of Yuan et al.[12] After crystallization of the inactivated enzyme, small crystals were collected and dissolved in 100 μL of water. The enzyme was denatured by addition of 2.5 volumes of ethanol and the NAD/NADH composition determined as before.

Table 2: Rate and Equilibrium Constants from the Work of Porter and Boyd (*22*−*24*) for the Catalytic Cycle and Abortive Reactions of Bovine AdoHcy Hydrolase Action at pH 7 and 25 °C[a]

constant	notation of Porter and Boyd	value of constant	ΔG,[b] kJ/ mol	reaction described
		Catalytic Cycle		
$k_{fs}/k_{ns} = K_S$	K_7	70 μM	−11	dissociation of S: $C^+\cdot S \leftrightarrow O^+ + S$
k_{os}	k_{-6}	107 s^{-1}	61	oxidation of S to KS: $C^+\cdot S \rightarrow C^0\cdot KS$
k_{rs}	k_6	25 s^{-1}	65	reduction of KS to S: $C^0\cdot KS \rightarrow C^+\cdot S$
k_{eh}	k_{-5}	3.5 s^{-1}	70	elimination of H from KS: $C^0\cdot KS \rightarrow C^0\cdot DK\cdot H$
k_{ah}	k_5	11 s^{-1}	67	addition of H to form KS: $C^0\cdot DK\cdot H \rightarrow C^0\cdot KS$
$k_{fh}/k_{nh} = K_H$	K_4	230 μM	−13	dissociation of H: $C^0\cdot DK\cdot H \leftrightarrow C^0\cdot DK + H$
k_{aw}	k_{-3}	9 s^{-1}	68	addition of H_2O to form KA: $C^0\cdot DK + H_2O \rightarrow C^0\cdot KA$
k_{ew}	k_3	28 s^{-1}	65	elimination of H_2O from KA: $C^0\cdot KA \rightarrow C^0\cdot DK + H_2O$
k_{oa}	k_2	83 s^{-1}	62	oxidation of A to KA: $C^+\cdot A \rightarrow C^0\cdot KA$
k_{ra}	k_{-2}	11 s^{-1}	67	reduction of KA to A: $C^0\cdot KA \rightarrow C^+\cdot A$
$k_{fa}/k_{na} = K_A$	K_1	9 μM	−5	dissociation of A: $C^+\cdot A \leftrightarrow O^+ + A$
		Abortive Reactions		
k_{rd}	k_{-8}	1.5×10^{-3} s^{-1}	89	abortive reduction of DK: $C^0\cdot DK \rightarrow C^+\cdot D$
k_{od}	k_8	0.087 s^{-1}	79	oxidation of D: $C^+\cdot D \rightarrow C^0\cdot DK$
k_{fka}	k_{-12}	4×10^{-7} s^{-1}	110	abortive release of KA: $C^0\cdot KA \rightarrow C^0 + KA$
k_{nka}	k_{12}	610 $M^{-1}s^{-1}$	91	reassociation of KA: $C^0 + KA \rightarrow C^0\cdot KA$

[a] See Figure 3 for notation [b] Standard Gibbs free energies of reaction for equilibria and of activation for rate processes; standard-state concentrations of 10^{-6} M.

RESULTS

The Complex of Human Placental AdoHcy Hydrolase with 3′-Keto-NepA Has a Closed Structure. Figure 2 shows the domain organization of a monomeric subunit of human placental AdoHcy hydrolase containing 3′-keto-NepA bound in the substrate-binding domain [catalytic domain (*1*, *8*)] and the cofactor in the reduced (NADH) state bound in the cofactor-binding domain (only NADH was present, as determined by the fluorescence technique described above). The structure closely resembles the closed-form structure originally observed (*8*) for the complex of the human placental enzyme (NADH as cofactor) with the keto form of a different inhibitor, DHCeA. The rms deviation between the present structure and the DHCeA-complexed structure (PDB code 1A7A) is 0.25 Å for all main chain atoms. The binding of DHCeA (PDB code 1A7A) and that of NepA are virtually identical, with the exception that the CH_2OH group on the carbocyclic ring (i.e., the only difference in structure between NepA and DHCeA) replaces the two water molecules defined as waters A and B in the DHCeA active site. Hence, the interactions of NepA with Asp 131, His 301, and His 55 are somewhat different from those with DHCeA.

The new structure also generally resembles the closed-form structures reported by Huang et al. (*25*) for the complex of the rat liver enzyme (NAD^+ as cofactor) with D-eritadenine, and by Komoto et al. (*26*) for a complex of the D244E mutant of the rat liver enzyme (NADH as cofactor) with 3′-ketoadenosine, in which the cofactor and substrate sites are occupied in about 50% of the molecules. Figure 2 also shows the open form of the enzyme (*9*), in which the substrate-binding domain and cofactor-binding domain are separated to expose the active site.

The Closed Form of AdoHcy Hydrolase Appears To Have a Longer Cofactor−*Substrate Distance Than the Open Form.* Superposition of the structures of the substrate-binding domains of the closed-form complexes of AdoHcy hydrolase upon the substrate-binding domain of the open form of the enzyme allows an estimation of changes in the position of the cofactor relative to bound substrate that may occur between the two structures. Docking studies (*28*) indicate the substrate to bind similarly in the open and closed structures. The particular distance of interest is that between C-3′ of the substrate and C-4′ of the cofactor, the distance over which hydride transfer must occur in the redox partial reaction.

The two cases of greatest significance involve the comparison of the open-enzyme structure with no ligand and NAD^+ as cofactor (PDB file 1KY4) to the closed-enzyme structure with 3′-keto-DHCeA as ligand and NADH as cofactor (PDB file 1A7A) or to the closed-enzyme structure with 3′-keto-NepA as ligand and NADH as cofactor (PDB file 1LI4, the structure reported in this paper). The distance between C-3′ of the substrate and C-4′ of the cofactor increases from 3.23 ± 0.58 Å (open form of the enzyme) to 3.64 ± 0.58 Å (closed form of the enzyme) in the comparison of 1KY4 to 1A7A, and from 3.37 ± 0.57 Å (open form of the enzyme) to 3.60 ± 0.57 Å (closed form of the enzyme) in the comparison of 1KY4 to 1LI4. The errors cited were calculated from the cross-correlated coordinate errors given in the PDB files (estimates were made by both the Luzzati and σ_A methods; the larger of the calculated estimates was used) or, when these were absent, from values provided by Professor F. Takusagawa. These structural comparisons are of greater significance than the other two, because the ligands DHCeA and NepA have both undergone oxidation at the 3′-position and both possess a trigonal carbon center at the 4′-position, thus making both of them analogues of the central intermediate 4′,5′-didehydro-5′-deoxy-3′-ketoadenosine. It is in the complex with this intermediate that an increase in the substrate−cofactor distance is of highest importance, because it decreases the rate of hydride transfer and abortive reduction (see below).

In the two cases that are less significant, the effect is nevertheless observed: the distance increases from 3.10 ± 0.46 to 3.54 ± 0.46 Å in the comparison of the open structure 1KY4 to the closed structure 1K0U and from 2.77 ± 0.48 to 3.22 ± 0.48 Å in the comparison of the open structure 1KY4 to the closed structure 1KY5. The errors were calculated as described above. These cases are of smaller

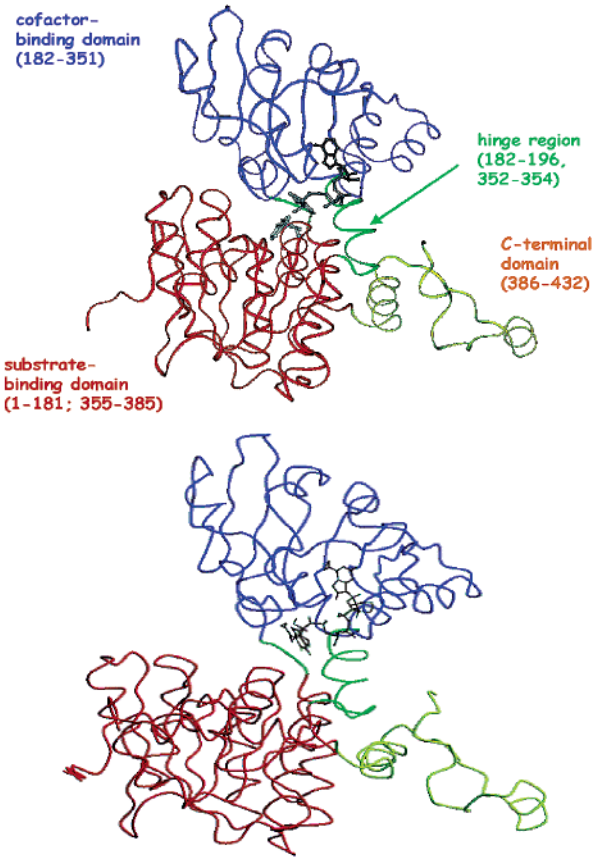

FIGURE 2: (Top) Domain organization in the closed-form structure of a monomeric subunit of the homotetrameric human placental AdoHcy hydrolase with the keto form of NepA and NADH (both black ball-and-stick figures) bound in the lower substrate-binding (red) and upper cofactor-binding (blue) domains, respectively. This organization is the same as that described by Turner et al. (*8*) for the human placental enzyme. Residues 1 and 2 are disordered in the structure and are not shown. The two large domains are linked by a hinge region (green). A smaller C-terminal domain (gold) extends into an adjacent monomeric subunit. The C-terminal domain of monomer A extends into monomer B, where it forms part of the cofactor-binding site of monomer B. Similarly, the C-terminal domain of monomer B extends into monomer A, where it forms part of the cofactor-binding site of monomer A. Monomers C and D have a similar relationship so that the homotetrameric structure is a dimer of dimers. (Bottom) Open structure of the enzyme (*9*) in which the two domains have now opened through an angle of 19° to expose the active site to the environment.

significance for the following reasons: (*1*) neither of the ligands in structures 1K0U and 1KY5 possesses a trigonal carbon at the 4′-position, so they do not resemble the central intermediate in this respect; (*2*) the ligand in structure 1K0U is an anionic, acyclic adenyl compound with non-ribose stereochemistry at the 2′/3′ positions, so it does not resemble the substrate, product, or intermediates; (*3*) the ligand and cofactor in structure 1KY5 are present at only partial occupancy in each of the active sites; (*4*) the enzyme in structure 1KY5 has undergone the D244E mutation, which severely impairs cofactor affinity.

The apparent increase in the distance from around 3.2 Å (open form) to around 3.6 Å (closed form) or about 0.4 Å is within the estimated error of about 0.7−0.8 Å for the difference of the two distances, making the magnitude of the change impossible to specify. However, the universal observation of an increase in the apparent distance suggests that this qualitative change is factual. That the cofactor has shifted in position between open and closed conformations is clear, the change in position of C-4′ being 0.81 ± 0.58 Å (1KY4/1A7A) or 0.68 ± 0.57 Å (1KY4/1LI4), but only about half this shift is projected onto the hydride-transfer vector.

The Closed Form of AdoHcy Hydrolase Has an Organized Chain of Water Molecules Linking the Active Site to the External Environment. The closed-form complex of AdoHcy hydrolase with 3′-keto-NepA possesses a chain of three localized water molecules (127, 129, and 238) with short O−O distances of 2.5−2.7 Å. These waters appear to be stabilized in place by interaction with the carboxylate group of Asp 182. The first molecule, water 127, is a short distance from the amido-Oδ of Asn 181 (3.4 Å) and of Asn 191 (3.6 Å), the amido-N centers of which are in turn close to the ϵ-amino group of Lys 186 (Asn 181, 2.6 Å; Asn 191, 2.7 Å), a probable acid−base catalyst of the catalytic chemistry. This array may serve to transport protons between the active site and the external environment in the closed form of the enzyme.

DISCUSSION

Chemistry and Enzyme Immobility Appear Correlated in the AdoHcy Hydrolase Catalytic Cycle. The structure reported here reinforces the developing picture of the linkage between the catalytic chemistry of AdoHcy hydrolase and the large-scale domain motion of the enzyme (*1*, *10*).

Figure 1 emphasizes, as described above, the overall division of the catalytic chemistry into two partial reactions, a redox partial reaction and an elimination/addition partial reaction, the former spanning the latter. In the substrate-free enzyme with the cofactor in the NAD^+ oxidation state, the substrate-binding domains execute an oscillatory motion (*10*) with a frequency of 4×10^7 s^{-1}, 40000-fold greater than the diffusional-encounter frequency of enzyme with 1 μM substrate (*27*). Yin et al. (*10*) showed that the oscillatory motion ceases upon binding of substrate or substrate analogues, including those that lack an oxidizable 3′-hydroxyl group. Recently, Huang et al. (*25*) also made the same suggestion, that binding without oxidation is sufficient to bring about closure of the enzyme.

Thus, a reasonable general model is that substrate binding initially occurs to the open form, with its easily accessible [although ill-fitting (*28*)] substrate-binding site. As the site is assembled about the loosely held substrate molecule, domain motion ceases. As the oxidation step occurs, it is possible that a number of further reorganization processes (see below) occur to achieve relatively rigorous isolation of the active site from the environment. Within the active site, thus isolated, the elimination/addition partial reaction takes place. Thereafter, as the reduction step generates the product molecule, it is again possible that a number of reorganization processes (the reverse of those at the oxidation step) take place. The enzyme opens, its affinity for the product is thereby removed, and product release can occur easily.

AdoHcy Hydrolase Is an Evolutionarily Advanced but Imperfect Enzyme. The general model just described can be expanded to the kinetic model shown in Figure 3, where microscopic rate constants are defined for each of the individual steps. We owe to Porter and Boyd (*22*−*24*) one of the most thorough and rigorous kinetic characterizations

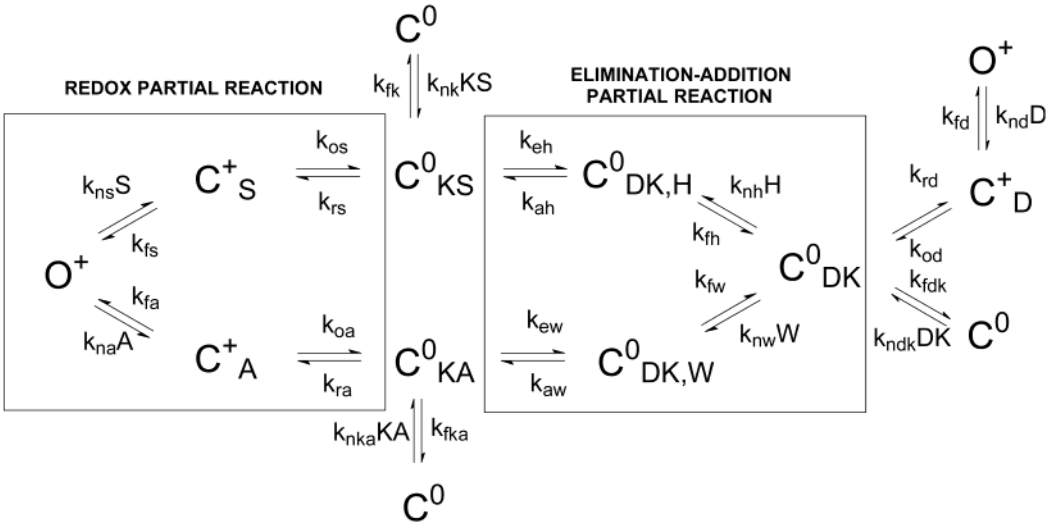

FIGURE 3: Notation for species and rate constants in the action of AdoHcy hydrolase. O denotes the open form and C the closed form of the enzyme, the superscripts + (NAD^+) and 0 (NADH) denote the oxidation state of the cofactor, and the subscripts denote the ligand present in the substrate binding site: S, AdoHcy; KS, 3′-keto-AdoHcy, DK, 4′,5′-didehydro-5′-deoxy-3′-ketoadenosine; D, 4′,5′-didehydro-5′-deoxyadenosine; H, homocysteine; W, water; KA, 3′-ketoadenosine; A, adenosine. Rate constants are denoted *k*, with an initial subscript indicating the nature of the reaction (n, on-reaction; f, off-reaction; o, oxidation; r, reduction; a, addition; e, elimination) and a second subscript identifying the reactant or product of the reaction (e.g., k_{os} and k_{rs}, oxidation of S and reduction to produce S; k_{eh} and k_{ah}, elimination of H and addition of H). All rate constants are written as first-order rate constants, second-order constants such as on-rate constants being multiplied by the appropriate concentration (e.g., k_{ns}S). Reactions and species within or between the two partial-reaction boxes form the productive catalytic cycle (hydrolysis of AdoHcy, clockwise; synthesis of AdoHcy, counterclockwise). Other processes are abortive: abortive release of KS (top), DK (right side), or KA (bottom) and abortive reduction of D to DK (right side).

of any enzyme system known, in which they determined reliable values of a very large number of rate and equilibrium constants for bovine AdoHcy hydrolase. Their microscopic rate constants generate values of the steady-state rate constants that are in good agreement with those we observe for the human placental enzyme. Table 2 gives the values they provide for rate and equilibrium constants used in the present paper and relates their notation to that of Figure 3; also given are values of the standard Gibbs free energy of reaction for equilibrium processes and of the standard Gibbs free energy of activation for rate processes. From these free-energy values, a plot of the free-energy barriers to reaction progress can be constructed, as shown in Figure 4. The standard-state concentrations of AdoHcy, Ado, and Hcy have been taken as 1 μM, which brings the overall free-energy change for the net reaction close to zero.

The plot of Figure 4 exhibits the characteristic phenomena of "thermodynamic matching" as described by Albery and Knowles (*29*). In Figure 4, the free energies of the transition states of physical steps (on- and off-reactions) are arbitrarily set at the diffusional limit and are shown in parentheses. The transition states of the chemical steps have all acquired approximately equal free energies, and the enzyme-bound reactant states are also matched with each other. This is the expected property of a catalyst that has been evolutionarily selected for increasing catalytic power (*29*). The limit of such evolution (enzymic perfection) is reached when the transition states of the chemical steps become lower in free energy than the transition states of the physical steps. The observation of isotope effects characteristic of the redox and elimination/addition partial reactions by Palmer and Abeles (*30*, *31*) confirms that, as in Figure 4, the transition states for the chemical steps possess higher free energies than those of the physical steps. The limit of perfection has not been reached in the evolution of AdoHcy hydrolase, which thus shows the expected features of an evolutionarily selected but still imperfect enzyme. A result of the thermodynamic matching that has been achieved is to bring the overall free-energy change for the redox steps close to zero, eliminating the effect of the redox potential of the cofactor on the rate of the redox reactions.

Some of the means by which AdoHcy hydrolase achieves the stabilization of its chemical transition states have recently been identified. Elrod et al. (*32*) have identified possible catalytic roles for several active-site residues by kinetic studies of mutant forms of the human placental enzyme. Closely related studies with the rat liver enzyme have now been reported by Takata et al. (*33*).

AdoHcy Hydrolase Avoids Abortive Release of the 3′-Keto Intermediates in the Elimination/Addition Partial Reaction by a Tight Closure of the Active Site Linked to the Redox Partial Reaction. Combination of the kinetic results of Porter and Boyd (*22*−*24*) with subsequent structural work now suggests that the oxidation reaction after substrate binding leads to a substantially increased barrier to ligand release and that this higher barrier persists until the final reduction reaction removes it, allowing rapid release of the product.

Porter and Boyd showed that binding and release of 3′-keto-Ado during the catalytic cycle occurred with rate constants that correspond (Figure 4) to a barrier of 110 kJ/mol for release. This barrier is around 50 kJ/mol higher than the diffusional limit, corresponding to a rate factor of 10^8 to 10^9. Thus, during the elimination/addition partial reaction, binding and release of ligands are slowed by many orders of magnitude relative to the diffusional limit. As can be seen from Figure 4, the decrease in the rate of ligand release does not arise in any major part from tighter binding of the substrate. The intermediate 3′-keto-Ado is bound by the enzyme only 5−11 kJ/mol more tightly than the rapidly

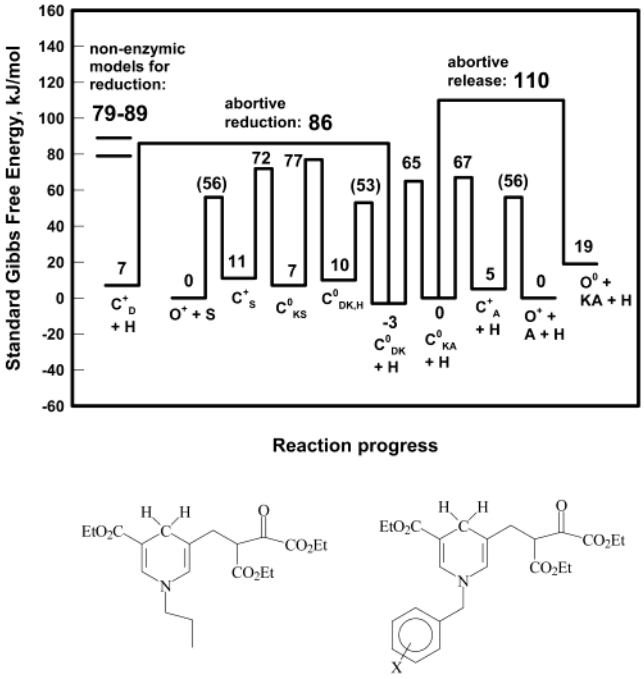

Model compounds of Kirby and Walwyn (*34, 35*) for non-enzymic hydride transfer from NADH to ketonic groups

FIGURE 4: Free-energy barriers in the catalytic cycle of AdoHcy hydrolase and for abortive reduction and abortive release of intermediates. Values were calculated from the rate constants of Table 2 for standard-state concentrations of 1 μM relative to the free energy of free enzyme and free AdoHcy. Barriers to normal ligand release are arbitrarily assigned a diffusional free energy (given in parentheses). The barrier to release of 3′-ketoadenosine is 110 kJ/mol, more than 50 kJ/mol greater than a diffusional barrier, corresponding to a rate-reduction factor of 10^{8-9}. This protective measure is presumably achieved by "sealing" of the active site. The barrier to abortive reduction is 89 kJ/mol, with a transition-state free energy of 86 kJ/mol relative to that of the reactant at −3 kJ/mol. This is a larger barrier than for productive reduction of 3′-ketoAdoHcy (65 kJ/mol) or 3′-ketoAdo (67 kJ/mol) by 22−24 kJ/mol, corresponding to a decrease in rate of 10^4-fold. Below the diagram are shown model systems of Kirby and Walwyn for intramolecular redox reactions of NADH with ketones. The *n*-propyl compound at the left undergoes the intramolecular reduction reaction in aqueous solution at 39 °C with a rate constant in the pH 3−6 region of 3×10^{-3} s^{-1}, corresponding to a free-energy barrier of 92 kJ/ mol. The *n*-propyl compound at the left and the benzyl compounds at the right undergo a Mg^{2+}-catalyzed reaction in 20% dioxane−water at 39 °C. At saturating Mg^{2+} concentrations, the first-order rate constants are 1×10^{-1} s^{-1} (*n*-propyl; barrier 82 kJ/mol), 2.5×10^{-2} s^{-1} (X = H; barrier 86 kJ/mol), and 7×10^{-3} s^{-1} (X = *p*-Br; barrier 89 kJ/mol). The barrier to abortive reduction is thus bracketed by the barriers for simple, nonenzymic intramolecular reductions, suggesting that the enzyme has suspended its catalytic power for reduction except for that deriving from intramolecularity.

released substrates; this strength of binding would slow release by only a factor of 10^{1-2}, while the observed retardation is 10^{8-9}-fold.

This property of the enzyme is of high significance for its catalytic power. The 3′-keto intermediates of the elimination/addition partial reaction are chemically labile upon exposure to aqueous buffers so that release of such intermediates or even their exposure to the aqueous environment is likely to result in their destruction and abortion of the catalytic cycle. Apparently AdoHcy hydrolase has developed the subtle strategy of linking a "sealing and unsealing" of the active site to the oxidation and reduction reactions that begin and end the catalytic cycle to sequester the labile 3′-keto intermediates during the middle part of the cycle.

AdoHcy Hydrolase Avoids Abortive Reduction of the Central Intermediate by a Temporary Decrease of its Redox Catalytic Power during the Elimination/Addition Partial Reaction. The next event after substrate binding in AdoHcy hydrolase action is oxidation of the substrate at the 3′-position. The keto group thus generated renders the 4′-CH bond sufficiently acidic to allow the elimination of the 5′-substituent to proceed, and therafter activates the central intermediate 4′,5′-didehydro-5′-deoxy-3′-ketoadenosine toward Michael addition of the new 5′-substituent, thus completing the elimination/addition partial reaction. It is vital for completion of the catalytic cycle that the NADH cofactor, bound in immediate proximity to the central intermediate, not reduce it at the 3′-position. Such a reduction would convert the facile Michael addition into a simple unactivated olefinic addition reaction, effectively aborting the catalytic cycle.

Porter and Boyd (*23*) recognized and discussed this point, and were able to obtain rate constants for the abortive reduction of the central intermediate. Figure 4 displays the result, indicating that the barrier to the abortive event is 89 kJ/mol (transition-state free energy of 86 kJ/mol relative to the reactant-state free energy of −3 kJ/mol), compared to barriers of 65 (72 minus 7) kJ/mol for the productive reduction to form AdoHcy and 67 kJ/mol for the productive reduction to form Ado. The abortive process is thus deprived of 22−24 kJ/mol of net transition-state stabilization by the enzyme, corresponding to a loss in catalytic acceleration of 10^4-fold.

A useful point of comparison is the nonenzymic, intramolecular model reaction for NADH reduction of ketones created by Kirby and Walwyn (*34, 35*), the model compounds for which are also shown in Figure 4. Under various circumstances, these processes occur with barrier heights of 82−91 kJ/mol, so that their relative transition-state free energies in Figure 4 would be 79−88 kJ/mol, bracketing the value for the abortive reduction. In terms of rate constants, the model reactions exhibit values of $(3-100) \times 10^{-3}$ s^{-1} at 39 °C while the value for the enzymic abortive reduction (Table 2) is 1.5×10^{-3} s^{-1} at 25 °C. The enzyme apparently decreases its redox catalytic power during the elimination/addition partial reaction to such a degree that abortive reduction proceeds at the rate expected for simple, intramolecular nonenzymic reduction.

The means by which AdoHcy hydrolase may possibly remove this fraction of its redox catalytic power is suggested by the structural comparison shown in Figure 5. Here the cofactor position in the open form of the enzyme, with the cofactor in the NAD^+ oxidation state and no substrate present, is taken to simulate the cofactor position relative to the newly bound substrate in the immediately formed ternary complex before substrate oxidation. The position of the cofactor in the closed form of the enzyme (now NADH) is then found to be such that the C-4′ (cofactor)-to-C-3′ (substrate) distance, the distance across which the hydride-transfer redox reactions must occur, is larger after the oxidation reaction than it was before this reaction. The increase in this distance seems clear from the structures, being reproduced in each of the four comparisons presented

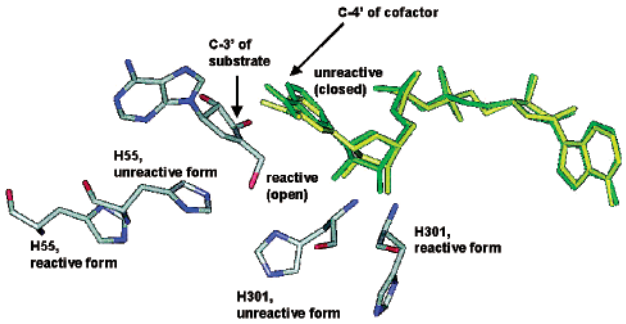

FIGURE 5: Conversion of the open, NAD^+ form of AdoHcy hydrolase to the closed, NADH form with keto substrate bound results in an increased distance for hydride transfer in the redox partial reaction, possibly explaining the 10^4-fold reduction in catalytic power for reduction during the elimination/addition partial reaction. Superposition of the structures of the open and closed forms of the enzyme indicates (a) a shift of the cofactor from the closer ("reactive") separation in the open form (yellow) to the more distant ("unreactive") position in the closed form (green) and (b) a change in the position of His 301 such that it buttresses the cofactor in the unreactive form. Changes in the locations of both His 301 and His 55 also bring them into an appropriate position for acid−base catalysis of addition and elimination reactions at C-5′ of the intermediate.

above. However, the apparent magnitude of the increase, which averages about 0.4 Å, is considerably smaller than the probable error in the coordinate differences, so the structural comparisons yield no information on the magnitude. The fact that the withdrawal of the cofactor from the ligand was observed not only for ligands that simulated the central intermediate (closed structures 1A7A and 1LI4) but also for structures with ligands that failed to simulate this intermediate suggests that the conformation change that suspends the catalytic power of the cofactor is coupled directly to domain−domain closure. Even if the closure is effected by an unusual ligand or by crystal packing forces, cofactor withdrawal occurs.

In addition to the apparent removal of the cofactor to a position more distant from the reducible intermediates, a shift in the position of His 301 occurs (Figure 5) so that it appears to buttress the cofactor in this more distant position. An oxidation-induced conformational change, in which the distance over which hydride transfer must occur in a redox reaction is increased, may therefore conceivably be the mechanism employed by AdoHcy hydrolase to "switch off" part of its redox catalytic power during the critical elimination/addition partial reaction. A reverse conformation change linked to the reduction reaction at the terminus of the catalytic cycle may then restore the catalytic power. If the redox reactions occur by a quantum-tunneling mechanism of hydride transfer, which may be regarded currently as the most likely mechanism (*36*, *37*), then a small increase in the hydride-transfer distance could readily produce a large increase in the free energy of activation because of the sensitivity of tunneling reactions to the tunneling distance. The changes in the positions of His 301 and also His 55, seen in Figure 5, serve the further purpose of placing these two residues in the neighborhood of C-5′ of the intermediate, where they may function as acid−base catalysts of the addition−elimination reactions (*1*).

AdoHcy Hydrolase May Maintain Active-Site Protonation States for Optimum Catalysis in the Closed Form of the Enzyme by Use of a Chain of Water Molecules for Export and Import of Protons. Acid−base catalysis of both partial reactions (*1*) in the closed form of the enzyme, when the active site is isolated from the external environment, poses a problem in the maintenance of the catalytic functional groups in the needed protonation states. Achievement of such control may require the export and import of protons between the solvent environment and the active site. A possible apparatus for this purpose can be seen in Figure 6: a chain of three water molecules leads from the site of acid−base catalysis to the surface of the enzyme. Studies are in progress to test this hypothesis.

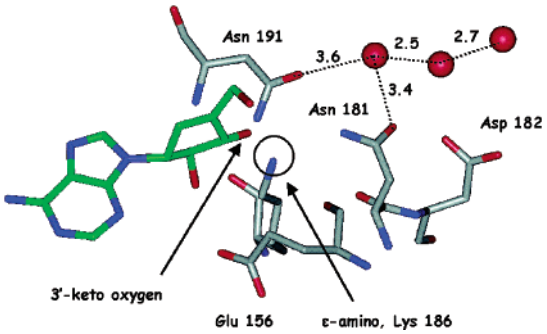

FIGURE 6: A chain of three water molecules (left to right, 127, 129, and 238 in the structure reported here), which may serve as a relay for the export and import of protons between Lys 186 and the external environment with the assistance of Asn 181 and Asn 191. Asp 182 appears suitably located to stabilize the positive charge as protons are moved along the chain. The O−O distances (Å) among the water molecules and the amido groups of Asn 181 and 191 are shown.

SUMMARY AND CONCLUSIONS

The model for the action of AdoHcy hydrolase that develops from the results described herein involves a linkage between conformational reorganizations of the enzyme and its catalytic functions. It was already known that substrate binding brings about a cessation of motion of the substrate-binding domain and formation of the closed structure without the necessity of substrate oxidation (*1*, *10*; see also ref *25*). We now suggest that the oxidation step produces a further structural change, which might speculatively be associated with the 14° rotation between the dimer pairs of the tetrameric structure described by Turner et al. (*1*). This change results in a sealing of the active site and the very high barrier to release of 3′-ketoAdo measured by Porter and Boyd (*22*−*24*). Doubtless, these conformation changes, particularly domain−domain closure, serve in part to organize the array of catalytic groups within the active site. Other 3′-keto intermediates, including the central intermediate 4′,5′-didehydro-5′-deoxy-3′-ketoadenosine, are also likely to be similarly protected from contact with the environment. A tunnel occupied by the Hcy moiety of AdoHcy (*1*) serves to permit release of the product Hcy (and possibly entrance of the water that will add across the 4′,5′-bond of the central intermediate) without opening of the active site. The tunnel appears unlikely, however, to admit the large amounts of water and buffer species necessary (*22*−*24*, *30*, *31*) to endanger the 3′-keto intermediates. The intermediates are further protected by close contacts about the ribose−adenine bond which is cleaved in the abortive hydrolysis reactions. Abortive reduction by the tightly bound NADH of the central

intermediate is avoided by temporary suspension of the redox catalytic power during the elimination/addition partial reaction, resulting in a decrease in reduction rates by a factor of 10^4. This decrease in reduction rate may be effected by an increase in the hydride-transfer distance that is produced when the sealing event occurs; a change in the position of His 301 may allow it to buttress the cofactor in its unreactive position. Redox catalytic power is then restored when the catalytic cycle terminates with reduction to generate the product, linked to the conformational change that "unseals" the active site and permits active-site opening and product release. Maintenance of ionizable active-site residues in catalytically suitable protonation states ("proton management") in closed forms of the enzyme may be assisted by a water chain, stabilized by Asp 182, that can import and export protons from and to the environment.

REFERENCES

1. Turner, M. A., Yang, X., Yin, D., Kuczera, K., Borchardt, R. T., and Howell, P. L. (2000) Structure and function of S-adenosylhomocysteine hydrolase, *Cell Biochem. Biophys. 33*, 101−125.
2. Schnyder, G., Roffi, M., Pin, R., Flammer, Y., Lange, H., Eberli, F. R., Meier, B., Turi, Z. G., and Hess, O. M. (2001) Decreased rate of coronary restenosis after lowering of plasma homocysteine levels, *N. Engl. J. Med. 345*, 1593−1600.
3. Ashfield-Watt, P. A., Moat, S. J., Doshi, S. N., and McDowell, I. F. (2001) Folate, homocysteine, endothelial function and cardiovascular disease. What is the link? *Biomed. Pharmacother. 55*, 425−433.
4. Ueland, P. M., Refsum, H., and Brattstrom, L. (1992) Plasma Homocysteine and Cardiovascular Disease, in *Arteriosclerotic Cardiovascular Disease, Hemostasis and Endothelial Function* (Francis, R. B., Jr., Ed.) pp 183−196, Marcel Dekker, New York.
5. Kruman, I. I., Kumaravel, T. S., Lohani, A., Pedersen, W. A., Cutler, R. G., Kruman, Y., Haughey, N., Lee, J., Evans, M., and Mattson, M. P. (2002) Folic acid deficiency and homocysteine impair DNA repair in hippocampal neurons and sensitize them to amyloid toxicity in experimental models of Alzheimer's disease, *J. Neurosci. 22*, 1752−1762.
6. Robins, M. J., Wnuk, S. F., Yang, X., Yuan, C. S., Borchardt, R. T., Balzarini, J., and De Clercq, E. (1998) Inactivation of S-adenosyl-L-homocysteine hydrolase and antiviral activity with 5′,5′,6′,6′-tetradehydro-6′-deoxy-6′-halohomoadenosine analogues (4′-haloacetylene analogues derived from adenosine), *J. Med. Chem. 41*, 3857−3864.
7. Yang, X., and Borchardt, R. T. (2000) Overexpression, purification, and characterization of S-adenosylhomocysteine hydrolase from Leishmania donovani, *Arch. Biochem. Biophys. 15*, 272−280.
8. Turner, M. A., Yuan, C. S., Borchardt, R. T., Hershfield, M. S., Smith, G. D., and Howell, P. L. (1998) Structure determination of selenomethionyl S-adenosylhomocysteine hydrolase using data at a single wavelength, *Nat. Struct. Biol. 5*, 369−376.
9. Hu, Y., Komoto, J., Huang, Y., Gomi, T., Ogawa, H., Takata, Y., Fujioka, M., and Takusagawa, F. (1999) Crystal structure of S-adenosylhomocysteine hydrolase from rat liver, *Biochemistry 38*, 8323−8333.
10. Yin, D., Yang, X., Hu, Y., Kuczera, K., Schowen, R. L., Borchardt, R. T., and Squier, T. C. (2000) Substrate binding stabilizes S-adenosylhomocysteine hydrolase in a closed conformation, *Biochemistry 39*, 9811−9818.
11. Coulter-Karis, D. E., and Hershfield, M. S. (1989) Sequence of full length cDNA for human S-adenosylhomocysteine hydrolase, *Ann. Hum. Gen. 53*, 169−175.
12. Yuan, C. S., Yeh, J., Liu, S., and Borchardt, R. T. (1993) Mechanism of inactivation of S-adenosylhomocysteine hydrolase by (Z)-4′,5′-didehydro-5′-deoxy-5′-fluoroadenosine, *J. Biol. Chem. 268*, 17030−17037.
13. Turner, M. A., Dole, K., Yuan, C-S., Hershfield, M. S., Borchardt, R. T., and Howell, P. L. (1997) Crystallization and preliminary X-ray analysis of human placental S-adenosylhomocysteine hydrolase, *Acta Crystallogr., Sect. D 53*, 339−341.
14. Otwinowski, Z., and Minor, W. (1997) Processing of X-Ray diffraction data collected in oscillating mode, *Methods Enzymol. 276*, 307−326.
15. Brünger, A. T., Adams, P. D., Clore, G. M., DeLano, W. L., Gros, P., Grosse-Kunstleve, R. W., Jiang, J. S., Kuszewski, J., Nilges, M., Pannu, N. S., Read, R. J., Rice, L. M., Simonson, T., and Warren, G. L. (1998) Crystallography & NMR Systems: a new software suite for macromolecular structure determination, *Acta Crystallogr., Sect. D 54*, 905−921.
16. Pannu, N. S., and Read, R. J. (1996) Improved structure refinement through maximum likelihood, *Acta Crystallogr., Sect. A 52*, 659−668.
17. Brünger, A. T. (1992) Free *R* value: a novel statistical quantity for assessing the accuracy of crystal structures, *Nature 355*, 472−474.
18. Brünger, A. T., Krukowski, A., and Erickson, J. (1990) Slow-cooling protocols for crystallographic refinement by simulated annealing, *Acta Crystallogr., Sect. A 46*, 585−593.
19. Brünger, A. T., Kuryan, J. K., and Karplus, M. (1987) Crystallographic *R* factor refinement by molecular dynamics, *Science 235*, 458−460.
20. Jones, T. A., Zou, J.-Y., Cowan, S. W., and Kjeldgaard, M. (1991) Improved methods for binding protein models in electron density maps and the location of errors in these models, *Acta Crystallogr., Sect. A 47* (Part 2), 110−119.
21. Laskowski, R. A., MacArthur, M. W., Moss, D. S., and Thornton, J. M. (1993) PROCHECK: a program to check the stereochemical quality of protein structures, *J. Appl. Crystallogr. 26*, 283−291.
22. Porter, D. J., and Boyd, F. L. (1991) Mechanism of bovine liver S-adenosylhomocysteine hydrolase. Steady-state and pre-steady-state kinetic analysis, *J. Biol. Chem. 266*, 21616−21625.
23. Porter, D. J., and Boyd, F. L. (1992) Reduced S-adenosylhomocysteine hydrolase. Kinetics and thermodynamics for binding of 3′-ketoadenosine, adenosine, and adenine, *J. Biol. Chem. 267*, 3205−3213.
24. Porter, D. J. (1993) S-adenosylhomocysteine hydrolase. Stereochemistry and kinetics of hydrogen transfer, *J. Biol. Chem. 268*, 66−73.
25. Huang, Y., Komoto, J., Takata, Y., Powell, D. R., Gomi, T., Ogawa, H., Fujioka, M., and Takusagawa, F. (2002) Inhibition of S-adenosylhomocysteine hydrolase by acyclic sugar adenosine analogue D-eritadenine. Crystal structure of S-adenosylhomocysteine hydrolase complexed with D-eritadenine, *J. Biol. Chem. 277*, 7477−7482.
26. Komoto, J., Huang, Y., Gomi, T., Ogawa, H., Takata, Y., Fujioka, M., and Takusagawa, F. (2000) Effects of site-directed mutagenesis on structure and function of recombinant rat liver S-adenosylhomocysteine hydrolase. Crystal structure of D244E mutant enzyme, *J. Biol. Chem. 275*, 32147−32156.
27. Fersht, A. (1999) *Structure and Mechanism in Protein Chemistry*, p 159, W. H. Freeman, New York.
28. Hu, Y., Yang, X., Yin, D. H., Mahadevan, J., Kuczera, K., Schowen, R. L., and Borchardt, R. T. (2001) Computational characterization of substrate binding and catalysis in S-adenosylhomocysteine hydrolase, *Biochemistry 40*, 15143−15152.
29. Albery, W. J., and Knowles, J. R. (1976) Evolution of enzyme function and the development of catalytic efficiency, *Biochemistry 15*, 5631−5640.
30. Palmer, J. L., and Abeles, R. H. (1979) The mechanism of action of S-adenosylhomocysteinase, *J. Biol. Chem. 254*, 1217−1226.
31. Palmer, J. L., and Abeles, R. H. (1976) Mechanism for enzymatic thioether formation. Mechanism of action of S-adenosylhomocysteinase, *J. Biol. Chem. 251*, 5817−5819.
32. Elrod, P., Zhang, J., Yang, X., Yin, D., Hu, Y., Borchardt, R. T., and Schowen, R. L. (2002) Contributions of active-site residues to the partial and overall catalytic activities of human S-adenosylhomocysteine hydrolase, *Biochemistry 41*, 8134−8142.
33. Takata, Y., Yamada, T., Huang, Y., Komoto, J., Gomi, T., Ogawa, H., Fujioka, M., and Takusagawa, F. (2002) Catalytic mechanism of S-adenosylhomocysteine hydrolase: Site-directed mutagenesis of Asp-130, Lys-185, Asp-189, and Asn-190, *J. Biol. Chem. 277*, 22670−22676.
34. Kirby, A. J., and Walwyn, D. R. (1987) Intramolecular hydride transfer from a 1,4-dihydropyridine to an α-ketoester in aqueous solution. A model for lactate dehydrogenase, *Tetrahedron Lett. 28*, 2421−2424.

35. Kirby, A. J., and Walwyn, D. R. (1987) Effective molarities for intramolecular hydride transfer. Reduction by 1,4-dihydropyridines of the neighbouring α-ketoester group, *Gazz. Chim. Ital. 117*, 667−680.
36. Kohen, A., and Klinman, J. P. (1999) Hydrogen tunneling in biology, *Chem. Biol. 6*, R191−R198.
37. Knapp, M. J., Rickert, K., and Klinman, J. P. (2002) Temperature-dependent isotope effects in soybean lipoxygenase-1: correlating hydrogen tunneling with protein dynamics, *J. Am. Chem. Soc. 124*, 3865−3874.

BI0262350